

AD-A183 548

CLIMATE SENSITIVITY AND LONG-PERIOD TEMPERATURE
FLUCTUATIONS(U) MASSACHUSETTS INST OF TECH CAMBRIDGE
CENTER FOR METEOROLOGY A. J. E. N LORENZ MAR 87

1/1

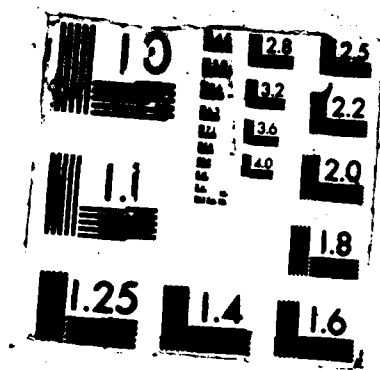
UNCLASSIFIED

AFGL-TR-87-0124 F19628-86-K-0001

F/G 4/2

NL





AFGL-TR-87-0124

Climate Sensitivity and Long-Period Temperature Fluctuations

Edward N. Lorenz

Massachusetts Institute of Technology
Center for Meteorology and Physical Oceanography
Cambridge, MA 02139

March 1987

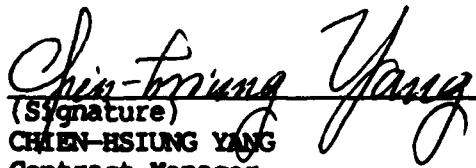
Final Report
4 March 1986-4 March 1987


Approved for public release; distribution unlimited

AIR FORCE GEOPHYSICS LABORATORY
AIR FORCE SYSTEMS COMMAND
UNITED STATES AIR FORCE
HANSCOM AIR FORCE BASE, MASSACHUSETTS 01731


DTIC
ELECTE
AUG 05 1987
S D
Ctd

"This technical report has been reviewed and is approved for publication"


(Signature)
CHIEN-HSIUNG YANG
Contract Manager


(Signature)
DONALD A. CHISHOLM
Branch Chief

FOR THE COMMANDER


(Signature)
ROBERT A. McCLATCHEY
Division Director

This report has been reviewed by the ESD Public Affairs Office (PA) and is releasable to the National Technical Information Service (NTIS).

Qualified requestors may obtain additional copies from the Defense Technical Information Center. All others should apply to the National Technical Information Service.

If your address has changed, or if you wish to be removed from the mailing list, or if the addressee is no longer employed by your organization, please notify AFGL/DAA, Hanscom AFB, MA 01731. This will assist us in maintaining a current mailing list.

Do not return copies of this report unless contractual obligations or notices on a specific document requires that it be returned.

Unclassified

A183540

SECURITY CLASSIFICATION OF THIS PAGE

REPORT DOCUMENTATION PAGE

1a. REPORT SECURITY CLASSIFICATION Unclassified			1b. RESTRICTIVE MARKINGS		
2a. SECURITY CLASSIFICATION AUTHORITY			3. DISTRIBUTION/AVAILABILITY OF REPORT Approved for public release distribution unlimited		
2b. DECLASSIFICATION/DOWNGRADING SCHEDULE					
4. PERFORMING ORGANIZATION REPORT NUMBER(S)			5. MONITORING ORGANIZATION REPORT NUMBER(S) AFGL-TR-87-0124		
6a. NAME OF PERFORMING ORGANIZATION Massachusetts Inst of Technology Ctr for Meteorology & Physical Oceanography		6b. OFFICE SYMBOL (If applicable)	7a. NAME OF MONITORING ORGANIZATION Air Force Geophysics Laboratory		
6c. ADDRESS (City, State and ZIP Code) Cambridge, MA 02139			7b. ADDRESS (City, State and ZIP Code) Hanscom AFB Massachusetts 01731		
8a. NAME OF FUNDING/SPONSORING ORGANIZATION		8b. OFFICE SYMBOL (If applicable)	9. PROCUREMENT INSTRUMENT IDENTIFICATION NUMBER F19628-86-K-0001		
8c. ADDRESS (City, State and ZIP Code)			10. SOURCE OF FUNDING NOS.		
			PROGRAM ELEMENT NO.	PROJECT NO.	TASK NO.
			61101F	ILIR	6E
11. TITLE (Include Security Classification) Climate Sensitivity and Long-Period Temperature Fluctuations			WORK UNIT NO. AA		
12. PERSONAL AUTHOR(S) Edward N. Lorenz					
13a. TYPE OF REPORT Final Report		13b. TIME COVERED FROM 3/4/86 TO 3/4/87		14. DATE OF REPORT (Yr., Mo., Day) 1987 March	
15. PAGE COUNT 24					
16. SUPPLEMENTARY NOTATION This research was supported by the Inhouse Laboratory Independent Research Fund					
17. COSATI CODES			18. SUBJECT TERMS (Continue on reverse if necessary and identify by block number)		
FIELD	GROUP	SUB. GR.			
			Low-order atmospheric models		
			Climatic fluctuations		
19. ABSTRACT (Continue on reverse if necessary and identify by block number) A special low-order moist general-circulation model is found to produce long-period fluctuations in the globally averaged atmospheric temperature, resembling the variations that have occurred in the real atmosphere. We propose that the fluctuations in the model, and possibly some of those in the atmosphere, occur because the sensitivity of the diabatic heating to temperature is highly variable. We construct a much simpler model, in which the diabatic heating is given by a simple function of temperature and local planetary temperature that approximates the diabatic heating in the original model, while the advective temperature changes are represented by random numbers. The new model produces similar long-period temperature fluctuations, thereby tending to support our hypothesis.					
20. DISTRIBUTION/AVAILABILITY OF ABSTRACT UNCLASSIFIED/UNLIMITED <input type="checkbox"/> SAME AS RPT. <input type="checkbox"/> DTIC USERS <input type="checkbox"/>			21. ABSTRACT SECURITY CLASSIFICATION Unclassified		
22a. NAME OF RESPONSIBLE INDIVIDUAL Chien-Hsiung Yang			22b. TELEPHONE NUMBER (Include Area Code) 617-377-3913		22c. OFFICE SYMBOL AFGL/LYP

TABLE OF CONTENTS

	PAGE
1. Introduction	1
2. The Model	5
3. The Experiments	9
4. Conclusions	11
References	12
Figure Captions	13

Accession For	
NTIS CRA&I	<input checked="" type="checkbox"/>
DTIC TAB	<input type="checkbox"/>
Unannounced	<input type="checkbox"/>
Justification	
By	
Distribution /	
Availability Codes	
Dist	Avail at 3 / or Special
A-1	



1. Introduction

The bulk of the atmosphere, the upper layers of the oceans and continents, and the ice, snow, and other material that often cover these layers, may be said to make up the climate system. Processes that influence the system but are not in turn influenced by it may be considered external. If a climate has become established, a subsequent small change in some external condition should lead in due time to the establishment of a new climate, probably differing slightly from the earlier one. For example, a small increase in solar output, represented perhaps by a 0.2-degree increase in the average planetary temperature T_0^* --the average temperature that the earth would acquire if it were a black body in radiative equilibrium with the sun--might actually cause a 0.5-degree increase in the global mean sea-level temperature T_0 , because of the greenhouse or some other effect. In such a case we would say that the *sensitivity* of T_0 to T_0^* is 2.5 (degrees per degree). We can also speak of the sensitivity of one quantity to a dimensionally different quantity--for example, the sensitivity of globally averaged rainfall to T_0^* , or the sensitivity of T_0 to atmospheric carbon dioxide content.

Under suitable circumstances the sensitivity of one quantity to another may be infinite, i.e., an infinitesimal change in some condition may induce a finite response. Infinite sensitivity is especially likely to be found in idealized models. Fig. 1, for example, is based on a low-order moist hemispheric-circulation model which was developed under a succession of contracts with AFGL; for documentation, see Lorenz (1984). We shall refer to the model as \tilde{M} . The three curves show the values of the atmospheric sea-level temperature T that would be in equilibrium with the indicated values of the "local planetary temperature" T^* , for different values of one of the

controllable parameters, when the horizontal variations of T^* have been suppressed.

In the model \tilde{M} , liquid water which has condensed in the atmosphere is carried along for a while before falling out as rain; clouds therefore have a "half-life" h . For the left-hand curve in Fig. 1, h has been set to 18 hours; a rather high sensitivity, peaking at about 6.0, occurs within a fairly limited range of T^* , centered near 267 K. For the middle curve h has been increased to 36 hours; we find two stable equilibrium values of T surrounding an unstable equilibrium when T^* lies in a very narrow range centered near 276 K. As the upper or lower limit of this range is approached from below or above, respectively, T becomes infinitely sensitive to an increase or decrease in T^* . For the right-hand curve, where h is 54 hours, the range of T^* for which there are multiple equilibria is considerably wider.

The high sensitivity occurring in \tilde{M} apparently results from a cloud-albedo feedback process. In \tilde{M} the albedo α has been made proportional to the cloud cover, which in turn is parameterized in terms of the relative humidity r . Although no relation between r and T is built into \tilde{M} , numerical solutions indicate that in general r is lower when T is higher. An increase in T^* will have the initial effect of increasing T ; the accompanying drop in r and hence in α allows more solar radiation to heat the earth, thus further increasing T . With a high value of h , when the atmosphere has difficulty in shedding its clouds, the cloud-albedo feedback process is enhanced. Auxiliary computations where α is held fixed, although r is allowed to vary, exhibit only finite sensitivity of T to T^* .

Fig. 2 shows the rate $\tilde{F}(T^*, T)$ at which T will vary in seeking equilibrium with a fixed T^* , for the case where $h = 36$ hours. Actually,

When all horizontal variations are suppressed, \tilde{M} retains three dependent variables--the total dew point W , the sea-surface temperature S , and T . When T^* is fixed, T , W , and S will ordinarily undergo three modes of variation. Two of these, characterized by rapid and sometimes oscillatory damping, represent mutual adjustments among T , W , and S . The third mode, which is the one depicted in Fig. 2, is characterized by slow damping, and represents a simultaneous adjustment of T , W , and S to T^* . In a typical time-dependent solution only the third mode is noticeable after a month or two. We shall treat \tilde{F} as the rate of diabatic heating, even though the more rapidly oscillating modes are also diabatic.

The zero line is of course the same as the middle curve in Fig. 1; the other isolines are somewhat similar in shape. The response can be very slow; sometimes many years are needed for T to come within one degree of equilibrium. For example, when $T^* = 278$ K, just above the range where infinite sensitivity exists, and T is initially low, say 250 K, T will at first appear to be slowing down toward an equilibrium at about 268 K. Only as T nears 268 K does it become apparent that T is not about to settle down there, and in due time T rises more rapidly, finally slowing again and approaching a true equilibrium at 306 K.

There is no compelling evidence that the cloud-albedo feedback process encountered in \tilde{M} operates in a similar manner in the real atmosphere. Possibly some other real-world processes operate in this manner. In this report our interest will be in any process which can produce a high or perhaps infinite sensitivity under a restricted set of external or internal conditions.

Fig. 3 shows the variations of T_0 for a 400-year numerical run made with \tilde{M} , starting with conditions that are compatible with the model's

climate (see also Lorenz, 1986). In this run the local planetary temperature T^* varies with latitude, but not with longitude nor time. The zonal flow produced by the cross-latitude heating contrast is baroclinically unstable, so that migratory waves develop, and transfer heat from one latitude to another. At any given latitude, T is generally not in equilibrium with T^* , and the diabatic effects represented by Fig. 2 are balanced in the long run by the advective temperature changes.

The total range of T_0 in Fig. 3 is somewhat greater than 2.0 K. Local fluctuations of this magnitude would be unspectacular, but the fluctuations in Fig. 3 are of global averages, and they seem to be at least comparable in magnitude to corresponding fluctuations in the real atmosphere during the past few centuries (cf. Fig. 3 of Hansen *et al.*, 1981). Certainly an almost monotone increase or decrease in the real atmosphere comparable to those beginning in Fig. 3 at years 32, 114, or 351 would, after progressing for a number of years, be interpreted by many investigators as a climatic change, and a cause would most likely be sought. In \tilde{M} the cause of these changes is purely internal; the external forcing, represented by T^* , undergoes no change with time.

Formally, the sensitivity $\sigma(T, T^*)$ of T to T^* is given by dT/dT^* , where the differentiation is performed under conditions of constant \tilde{F} . We may also speak of the sensitivities $\sigma(\tilde{F}, T^*)$ and $\sigma(\tilde{F}, T)$ of the rate of diabatic heating to T^* and T ; they are given by $\partial \tilde{F}(T^*, T)/\partial T^*$ and $\partial \tilde{F}(T^*, T)/\partial T$. It is evident that $\sigma(\tilde{F}, T) = -\sigma(\tilde{F}, T^*)/\sigma(T, T^*)$.

We now propose that the long-period fluctuations exhibited in Fig. 3 are related to the high climatic sensitivity $\sigma(T, T^*)$ and its restriction to a limited range, which assures us of a highly variable sensitivity, although the high heat capacity of the oceanic mixed layer, set at ten times that of

the atmosphere, also plays a role. In brief, the internal advective processes do not alter T_0 , but they can alter the values of T at two different locations by equal and opposite amounts. If some sort of equilibrium has been established, and if the values of $\sigma(\tilde{F}, T)$ at these locations are different, the alterations in the diabatic effects will not cancel, and the equilibrium will be upset. Since $\sigma(\tilde{F}, T^*)$ is not highly variable, large variations in the sensitivity $\sigma(T, T^*)$ imply variations in $\sigma(\tilde{F}, T)$.

To support our hypothesis we shall construct a model, which we shall call M , and which will be much simpler than \tilde{M} , but will nevertheless retain the essence of the processes believed to be important for the very-long-period fluctuations. The model M will, in fact, run four or five orders of magnitude faster than \tilde{M} , even though \tilde{M} is "low order." We shall then demonstrate that M can produce a curve very much like Fig. 3 when the sensitivity of diabatic heating to T varies considerably with T , but not when it is nearly constant.

2. The model

Our new model M has a single independent variable, time t , and two dependent variables, the temperatures T_1 and T_2 representing conditions in a low-latitude and a high-latitude belt. The planetary temperatures T_1^* and T_2^* at these latitudes are prespecified. The governing equations have the form

$$dT_1/dt = F(T_1^*, T_1) + G, \quad (1a)$$

$$dT_2/dt = F(T_2^*, T_2) - G, \quad (1b)$$

where F is a simple function that represents the diabatic effects and is supposed to approximate \tilde{F} , and G is a random variable that represents the advective processes and does not directly alter the mean temperature $T_0 = (T_1 + T_2)/2$.

Certain key points (T^*, T) in Fig. 2 have been designated by the letters A, B, C, D, E, P, Q. The point C is the inflection point of the zero line. Points B and D occur where the zero line has a vertical tangent, or $\sigma(F, T) = 0$, while A and E, also on the zero line, have the same T^* -coordinate as C. Points P and Q, on curves adjacent to the zero line, have the same T -coordinate as C. The function F contains several constants whose values may be assigned at will, so that F may look rather like or rather unlike \tilde{F} . We shall consider the optimum values of the constants to be those that produce the proper values of T^*_C , $T^*_B - T^*_D$, $T_E - T_A$, and $T_Q - T_P$; here a subscript refers to a designated point. However, we shall not insist that even the optimum values make F a truly close approximation to \tilde{F} .

To construct the function F , we note first that T^*_C and T_C are nearly equal in Fig. 2, and we neglect the difference. We note next that even though the climate sensitivity $\sigma(T, T^*)$ is considerably lower for low values of T in Fig. 2 than for high values, $\sigma(\tilde{F}, T^*)$ is also lower for low values of T ; as a consequence, $\sigma(\tilde{F}, T)$, whose variations we have presumed to be responsible for the long-term variations of T_0 , is about the same for low and high values of T , and the principal contrast is between the intermediate values of T , near T_C , and the values that are either high or low. We will not alter this feature if we do not recognize any departures of Fig. 2 from symmetry with respect to a 180° rotation about C, and in particular if we make $\sigma(F, T^*)$ a constant. A simple function satisfying our requirements is

$$F(T^*, T) = kU[\tau^* - \tau + b^2\tau/(1 + |\tau|)] , \quad (2)$$

where k is an inverse damping time, U is a temperature unit, $\tau = (T - T_c)/U$ is a dimensionless temperature, τ^* is defined analogously to τ , and b is a dimensionless parameter which affects the extent of the region of infinite sensitivity of T to T^* . The use of an absolute value in Eq.(2) introduces a discontinuity in the curvature of the zero line at C , but this does not appear troublesome. Functions such as $\arctan \tau$ or $\tanh \tau$ could have been used instead of $\tau/(1 + |\tau|)$.

The points A , B , D , and E exist when $b > 1$. Points B and D then occur where $d\tau^*/d\tau$ vanishes along the curve $F = 0$, while A and E occur where τ^* vanishes on this curve. Since $\tau < 0$ at A and B and $\tau > 0$ at D and E , we find that $\tau'_B = -\tau'_D = (b - 1)^2$, while $\tau_E = -\tau_A = b^2 - 1$. It follows that $(\tau_E - \tau_A)/(\tau'_B - \tau'_D) = (b + 1)/(b - 1)$. This allows us to determine an optimum value for b , after which an optimum value for U follows.

Fig. 4 is similar in format to Fig. 2, and it shows the field of $F(T^*, T)$, which is supposed to simulate $\tilde{F}(T^*, T)$, when the constants have essentially their optimum values. The similarities of the two figures and also the differences are apparent.

Because the diabatic temperature changes are so slow, it will be feasible to integrate Eqs. (1) using uncentered forward differences, with a time step Dt that is supposed to be so large that the advective effects during successive steps are more or less independent. We shall therefore let

$$G = cUR , \quad (3)$$

where successive values of R are chosen at random from a uniform distribution with $-1 < R < 1$, and c is dimensionless. It might have been preferable to let R have a small negative mean value instead of a zero mean, since the advective processes should tend to reduce the horizontal temperature contrast $T' = (T_1 - T_2)/2$, but we shall not explicitly introduce this refinement, noting instead that adding a constant to R would be equivalent to changing T_1' and T_2' by equal and opposite amounts. In completely dimensionless form, the equations of M reduce to

$$D\tau_1 = a[\tau_1' - \tau_1 + b^2\tau_1/(1 + |\tau_1|)] + cR, \quad (4a)$$

$$D\tau_2 = a[\tau_2' - \tau_2 + b^2\tau_2/(1 + |\tau_2|)] - cR, \quad (4b)$$

where $a = kDt$.

Although τ_1 and τ_2 are supposed to be dynamically coupled, it is apparent from Eqs. (4) that the value of τ_2 has no effect upon the behavior of τ_1 , and vice versa. Hence two experiments, performed with the same values of τ_1' but different values of τ_2' , and with identical sequences of random numbers, would produce identical time series for τ_1 . We do not feel that this is a shortcoming. The advective processes, for which the random numbers are a substitute, not only affect τ_1 and τ_2 but are affected by τ_1 and τ_2 ; a pair of experiments with different values of τ_2' , and hence different behaviors of τ_2 , but with identical sequences of random numbers, would therefore have no meaningful physical interpretation, even though such experiments might prove useful for studying the properties of M .

When $\tau_1 > 0$ and $\tau_2 < 0$, we can rewrite Eqs. (4) in terms of τ_0 and τ' . We find that

$$D\tau_0 = a[\tau_0' - \tau_0 + b^2\tau_0/(1 + 2\tau' + \tau'^2 - \tau_0^2)], \quad (5a)$$

$$D\tau_1 = a[\tau_1' - \tau' + b^2(\tau' + \tau'^2 - \tau_0^2) / (1 + 2\tau' + \tau'^2 - \tau_0^2)] + cR. \quad (5b)$$

With $b = 0$, which would imply that $\sigma(T, T')$ is strictly constant, τ_0 would soon become permanently indistinguishable from τ_0' . With $b > 0$, however, τ_0 will never become steady (unless $\tau_0' = 0$), since it will be affected by τ' , which will continue to vary because of the random advective forcing.

3. The experiments

In our numerical experiments with M we shall choose $Dt = 7.2$ days, or 0.02 years, as a reasonable time interval separating essentially independent baroclinic events. In the first experiment we shall use essentially optimum values for the constants that appear in F. From Fig. 2 (actually from the numerical output used in constructing Fig. 2) we observe that, approximately, $T_c = T_c' = 276$ K, $T_b' - T_d' = 1.4$ K, $T_E - T_A = 35$ K, and $T_Q - T_P = 20$ K. It follows that $b = 1.083$, whence $U = 100.8$ K. Since the values of F on the lines adjacent to the zero line in Fig. 2 are $+ 20$ K/year, $1/k = 6$ months, so $a = 0.04$. We shall let $c = 0.01$, thus implying that the advective processes can raise or lower T' by as much as 1.0 K per 7.2-day time step--a not unreasonably high value (cf. Eq. 28 of Stone et al., 1982).

Anyone performing experiments with Eqs. 4 will soon discover that the general behavior depends crucially on the values of T_1^* and T_2^* . Since the model recognizes distinct temperatures at only two points, we cannot expect to produce the needed contrast between the values of $\sigma(F,T)$ at these points unless one temperature is near T_c , while the other is decidedly higher or lower. This is most likely to happen if one planetary temperature is near T_c , while the other is not. Accordingly, in our experiments we shall let $\tau_1^* = 0.1$ and $\tau_2^* = -0.01$, implying that $T_1^* = 286$ K and $T_2^* = 275$ K.

We begin with the essentially optimum values $a = 0.04$, $b = 1.08$, $c = 0.01$, $T_c = 276$ K, and $U = 100$ K. Fig. 5 is constructed like Fig. 3, and it shows the variations of annual averages of T_0 produced by M for 400 consecutive years. The initial conditions were chosen arbitrarily, and the solution was run for 20 years before the start of Fig. 5.

The qualitative resemblance of the figures is apparent, even though not complete. As in Fig. 3, there are many nearly steady increases or decreases of T_0 that resemble climate changes, although there are instances, particularly in the third and fourth centuries, when the trends fail to persist as long as ten years. Near the beginning and again near the end of the first century there are almost continual decreases of T_0 lasting about 20 years; the latter is followed by a more broken increase for about 35 years. The resemblance might be made even closer by effectively stretching the curves, perhaps by altering the values of the constants so that what took place in 400 years will require 600 years.

Further evidence that the time scales displayed in Fig. 5 are nearly right is provided by Fig. 6, which compares 100 consecutive 72-day or 0.2-year averages, 100 consecutive 1-year averages, and 100 consecutive 5-year

averages. Only the middle curve looks like Fig. 3; 72-day averages are much too persistent, while 5-year averages are not persistent enough.

In Fig. 7 we present 100-year runs with $b^2 = 0.6, 0.8, 1.0, 1.2$, and 1.4 , while the remaining constants are as before. As anticipated, the smallest value of b^2 does not produce large-amplitude fluctuations of T_0 , and the fluctuations that do occur do not seem to favor long periods. The amplitude is greatest when $b = 1.0$, where infinite sensitivity of T to T^* is just appearing. It may seem surprising that the amplitude is smaller again when $b^2 = 1.4$, where infinite sensitivity is well established, but we can explain this by noting that, in the figure that would replace Fig. 4 when $b^2 = 1.4$, with curves that are more strongly S-shaped, the zero line and the vertical line $T^* = T_2^* = 275$ K would intersect at a value of T far below T_c , with a moderate value of $\sigma(T, T^*)$. There is also a second stable equilibrium value of T_2 when $b^2 = 1.4$, considerably higher than T_c ; our experiments were performed with T_2 oscillating about the lower equilibrium value.

We conclude from these experiments that contrasting values of $\sigma(F, T)$, the sensitivity of the rate of diabatic heating to temperature, are essential if long-period variations of T_0 are to be produced by M , or by a model that includes only those physical processes simulated by M .

4. Conclusion

We have seen that a low-order model of a moist general circulation can generate long-term variations of the globally averaged temperature, bearing a resemblance to climatic fluctuations, even when the external influences undergo no variations with time. The variations depend upon a cloud-albedo feedback process that develops in the model. We have also seen that a much

simpler model, in which the baroclinic processes are represented by a sequence of random numbers, can generate similar long-term variations.

Our point is not that long-period fluctuations can be produced by a perhaps unrealistic cloud-albedo feedback process. It is that they may be produced by any process or combination of processes that can make the sensitivity of diabatic heating to temperature highly variable.

In effect, we have uncovered an apparently overlooked mechanism, to be added to a long list of known or suspected mechanisms, for producing long-period atmospheric variations. Whether this mechanism is present in the real atmosphere or the real climate system, and, if it is, what the specific processes that enter the mechanism may be, we are not presently in a position to say.

References

Hansen, J., D. Johnson, A. Lacis, S. Lebedeff, P. Lee, D. Rind, and G.

Russell, 1981: Climate impact of increasing atmospheric carbon dioxide. *Science*, 213, 957-966.

Lorenz, E. N., 1984: Formulation of a low-order model of a moist general circulation. *J. Atmos. Sci.*, 41, 1933-1945.

Lorenz, E. N., 1986: The index cycle is alive and well. *Namias Sympos.*, Scripps Inst. of Oceanography.

Stone, P. H., S. J. Ghan, D. Spiegel, and S. Rambaldi, 1982: Short-term fluctuations in the eddy heat flux and baroclinic stability of the atmosphere. *J. Atmos. Sci.*, 39, 1734-1746.

Figure Captions

Fig. 1. The equilibrium values of the sea-level temperature T , in degrees K, corresponding to values of the local planetary temperature T^* , in degrees K, for model \tilde{M} , when the half-life for clouds is 18 hours (left curve), 36 hours (center curve), and 54 hours (right curve).

Fig. 2. The diabatic heating rate $\tilde{F}(T^*, T)$, in K/year, corresponding to the indicated values of T^* and T , in degrees K, for model \tilde{M} , when the half-life for clouds is 36 hours. The points A, B, C, D, E, P, Q are key points used in calibrating the approximation F to \tilde{F} .

Fig. 3. The variations with time t , in years, of annual averages of the globally averaged sea-level temperature T_0 , in degrees K, produced by model \tilde{M} , for 400 successive years.

Fig. 4. The function $F(T^*, T)$, in K/year, serving as an approximation in the model M for the function \tilde{F} shown in Fig. 2.

Fig. 5. The same as Fig. 3, but for the model M , with $T_c = 276$ K, $U = 100$ K, $a = 0.04$, $b = 1.08$, and $c = 0.01$.

Fig. 6. The variations with t , in years, of 0.2-year averages (top curve), 1-year averages (middle curve), and 5-year averages (bottom curve) of T_0 , in degrees K, produced by M , with the conditions of Fig. 5.

Fig. 7. The variations with t , in years, of annual averages of T_0 , in degrees K, produced by M , with the conditions of Fig. 5, except that $b^2 = 0.6$ (top curve), 0.8 (next curve), 1.0 (middle curve), 1.2 (next curve), and 1.4 (bottom curve).

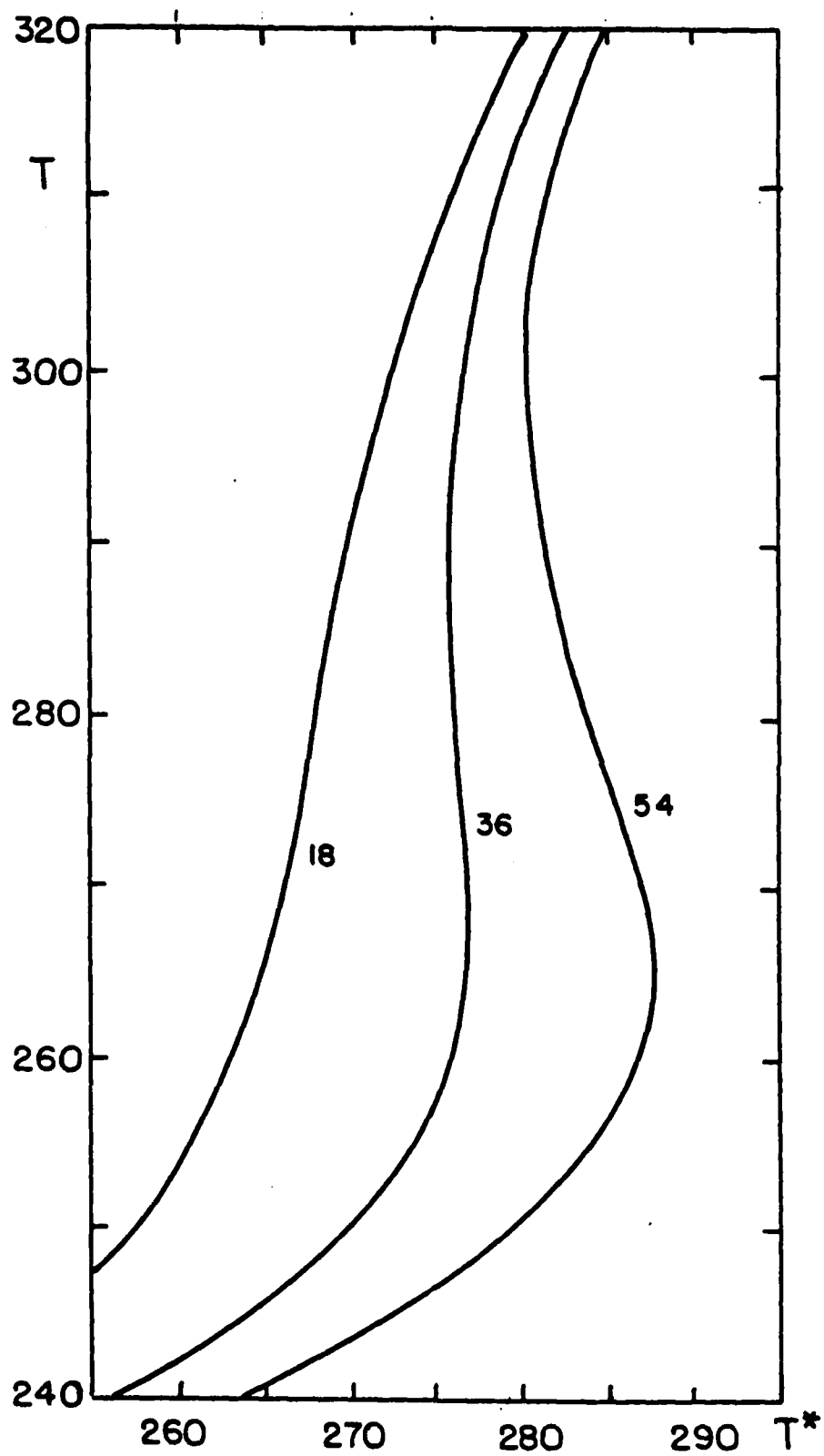


Figure 1

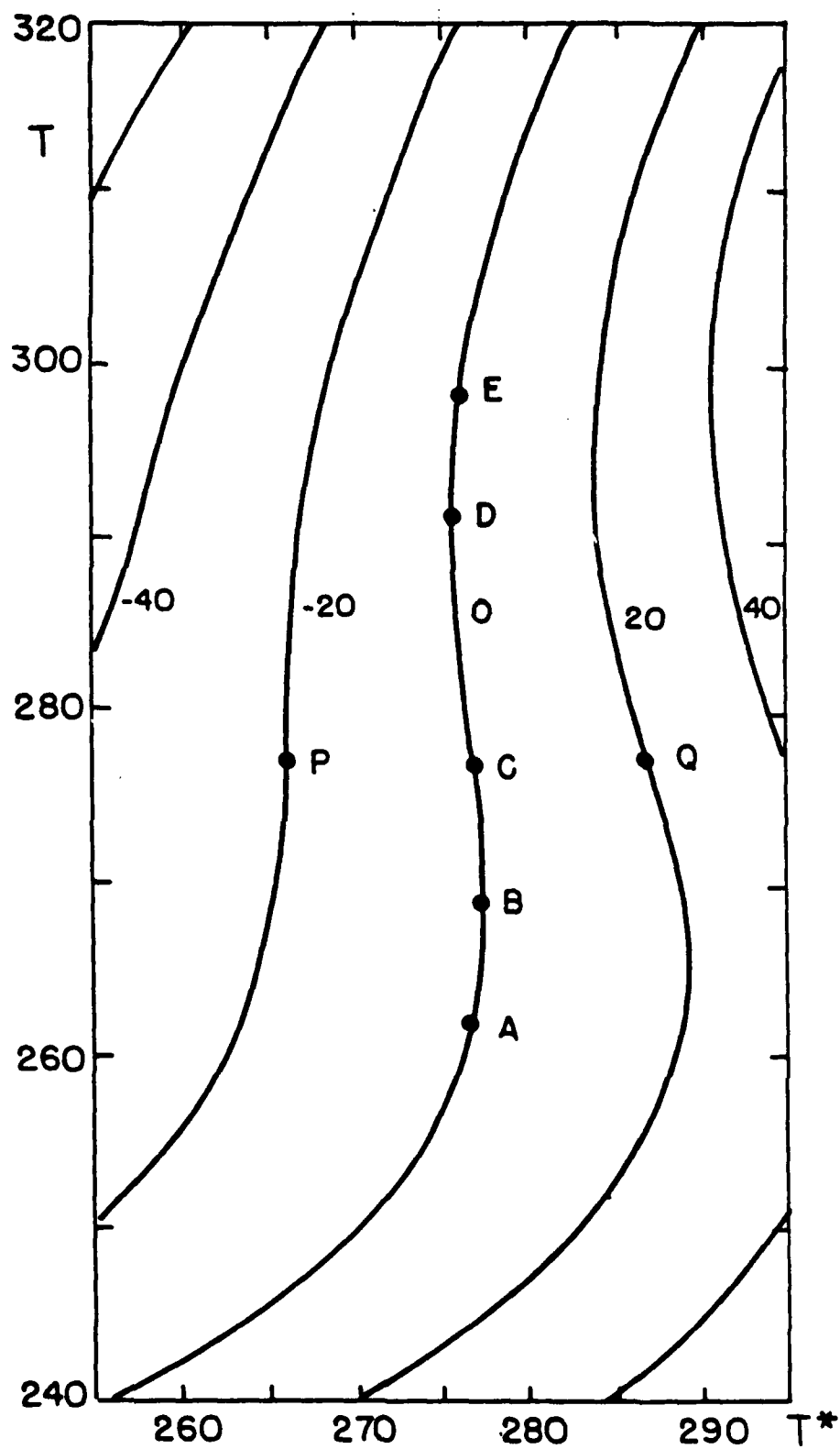


Figure 2

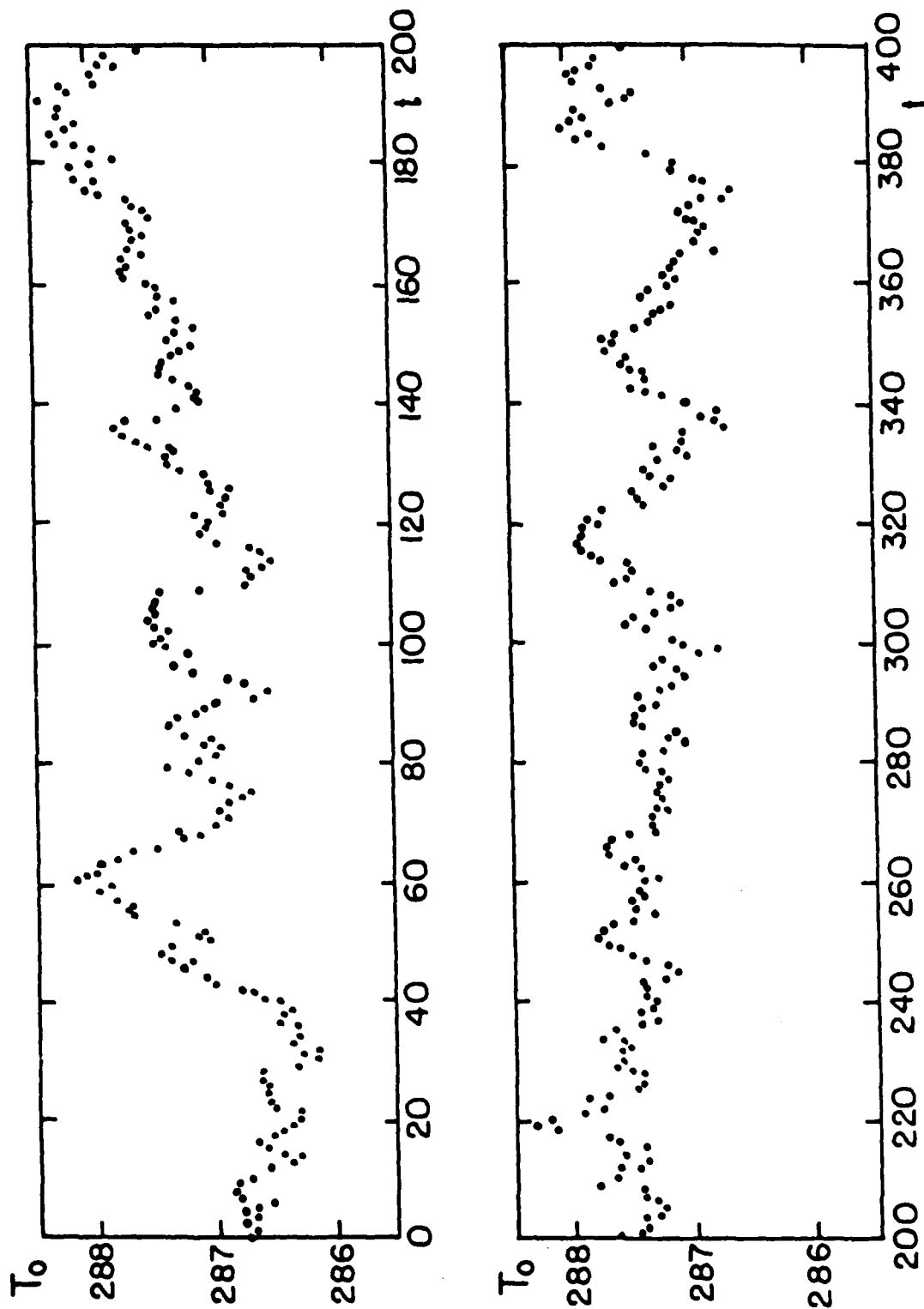


Figure 3

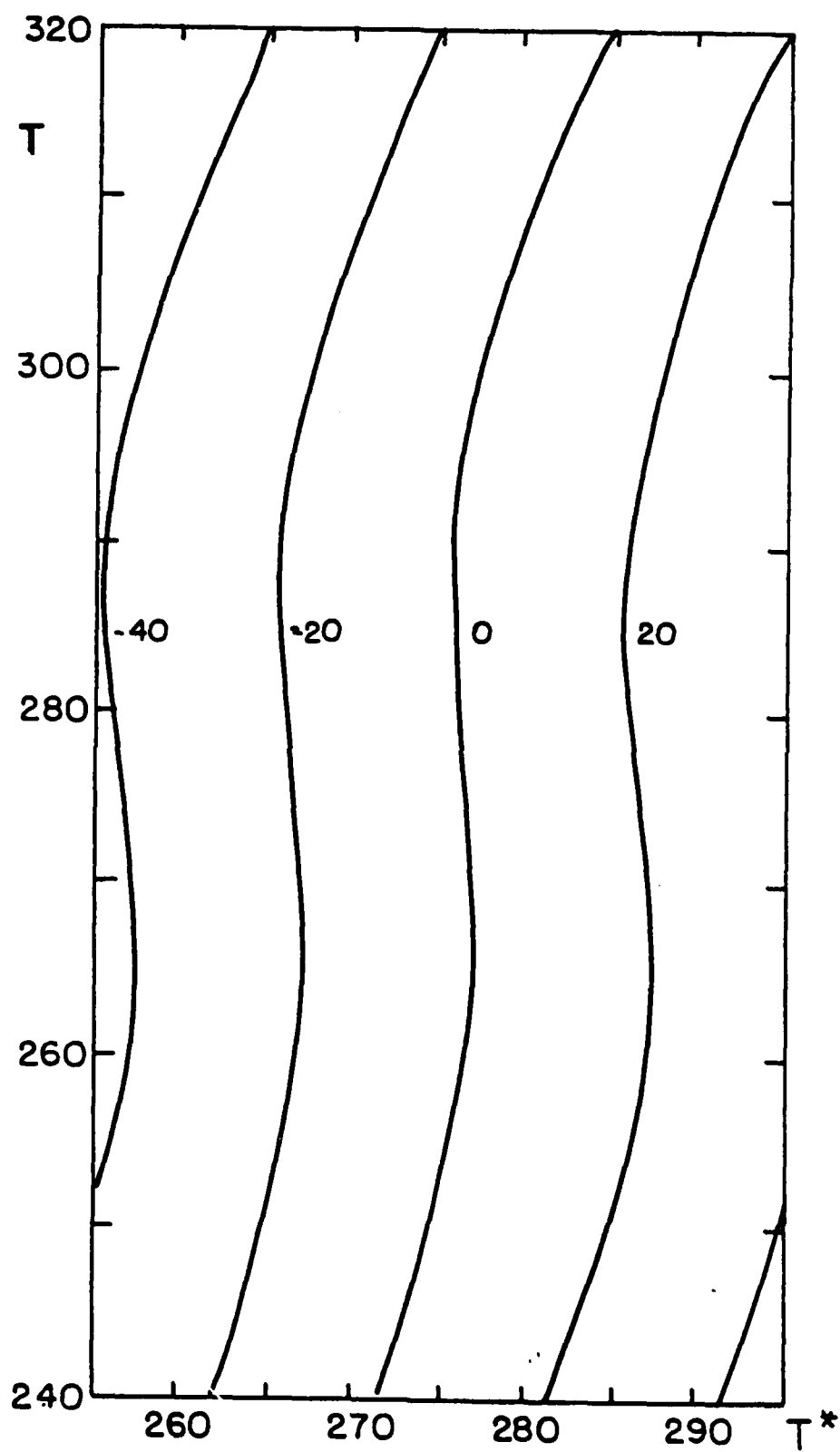


Figure 4

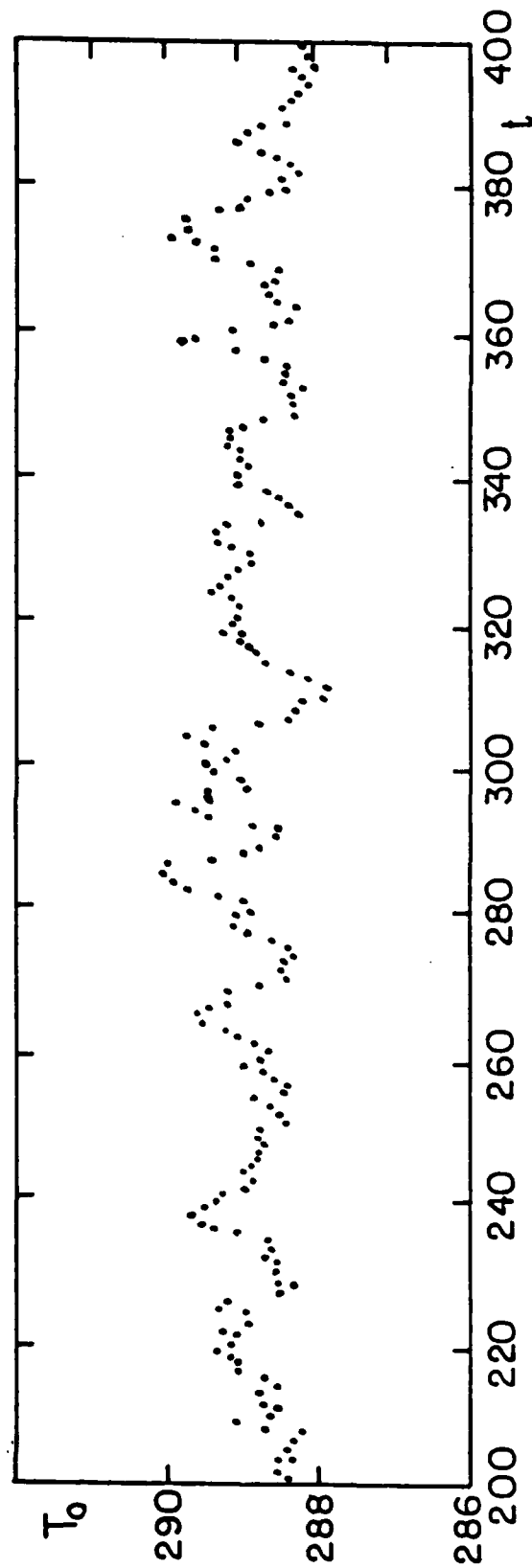
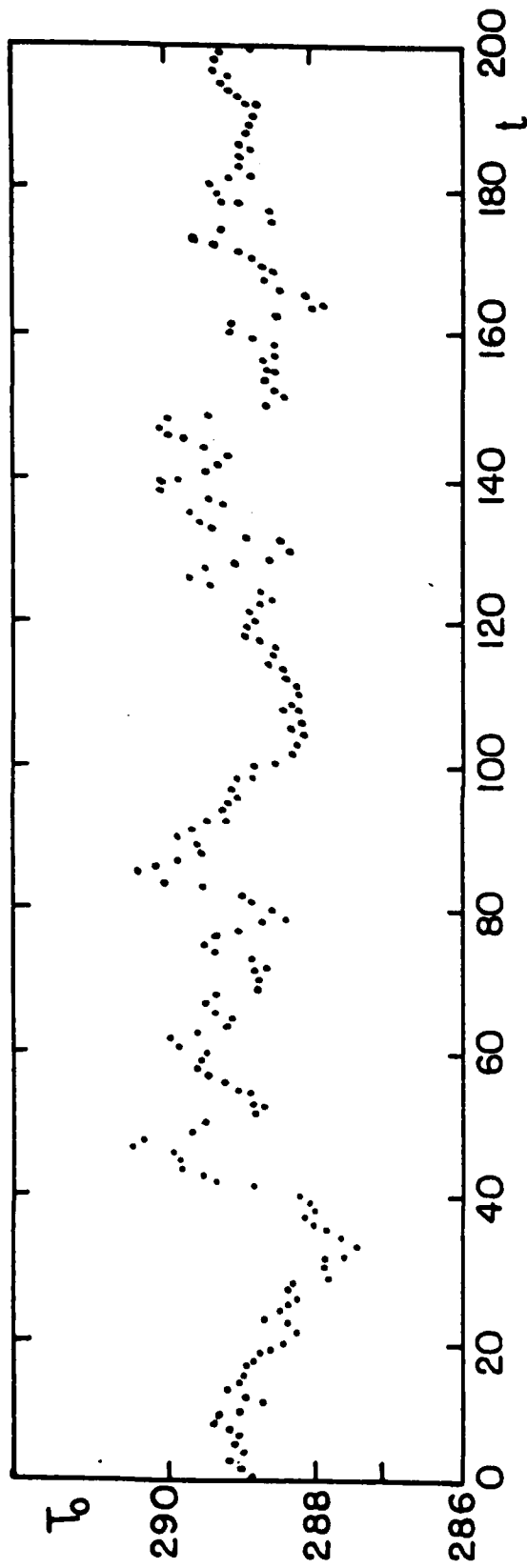


Figure 5

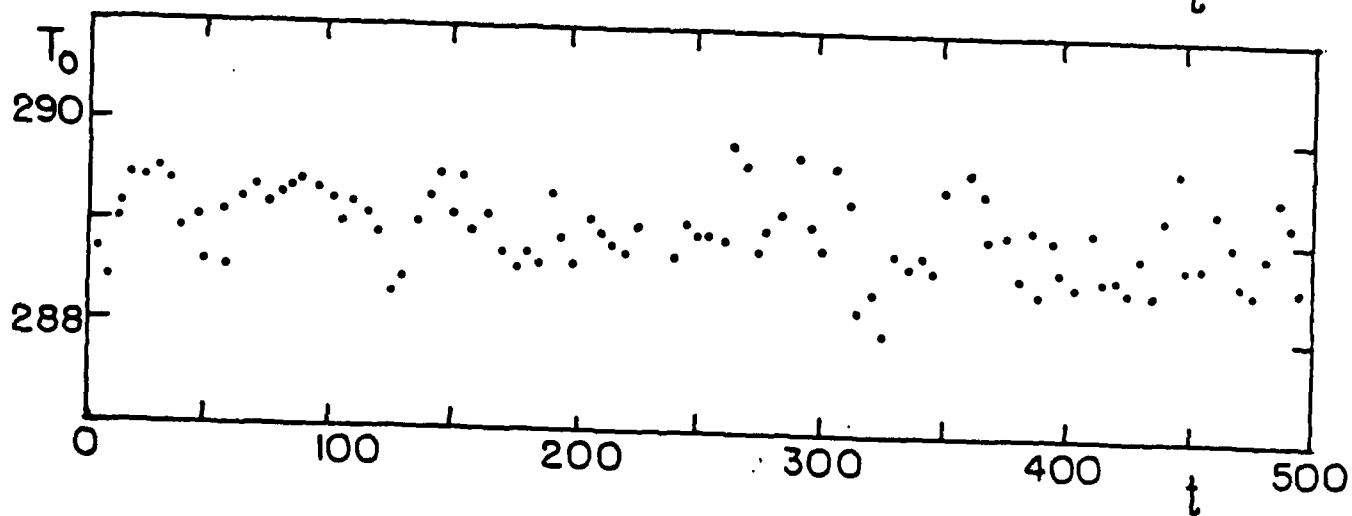
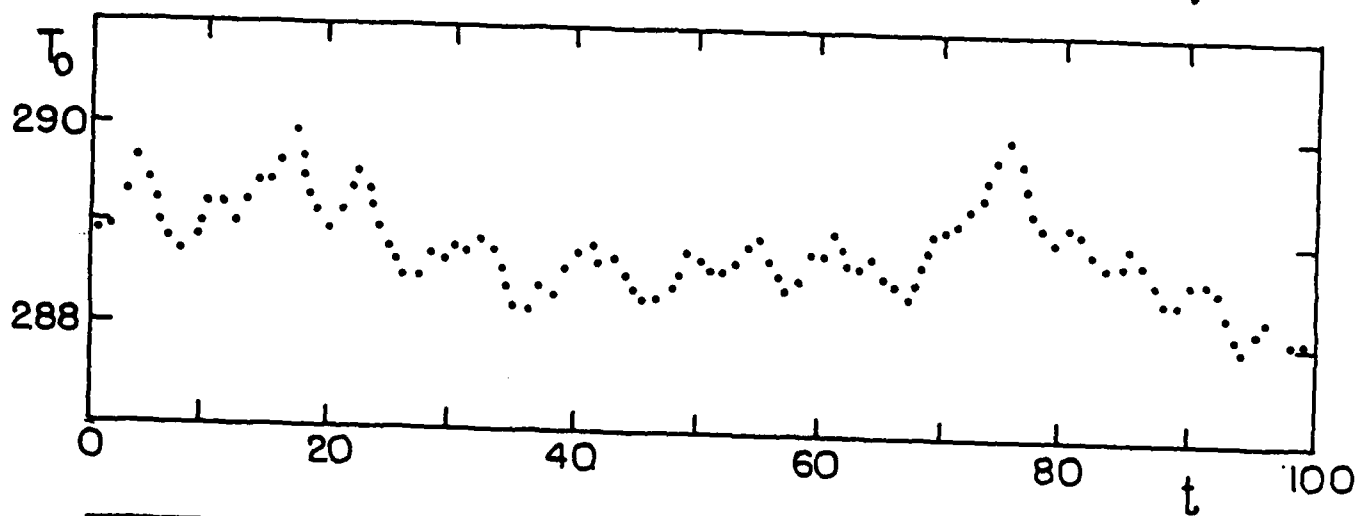
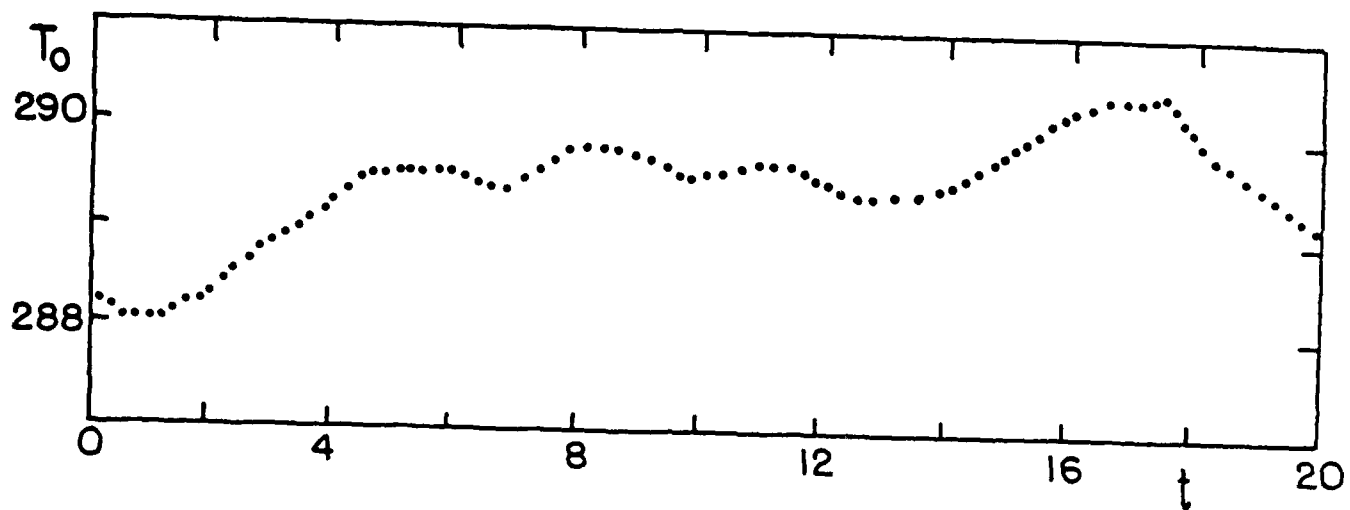


Figure 6

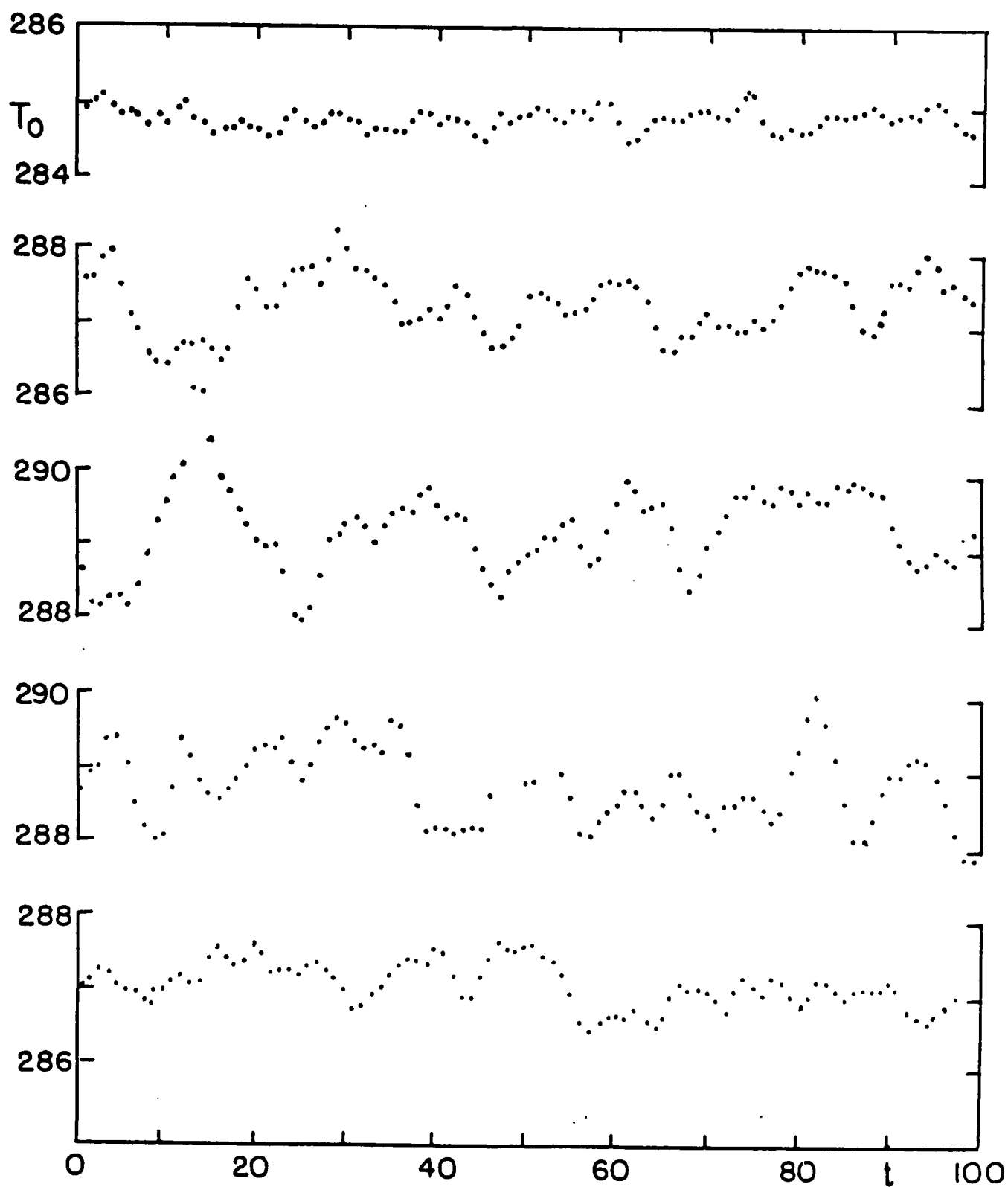


Figure 7

END

9-87

Dtic